Soft Matter

Cite this: *Soft Matter*, 2011, **7**, 7194

www.rsc.org/softmatter

COMMUNICATION

Polymers with hydro-responsive topography identified using high throughput AFM of an acrylate microarray†

Andrew L. Hook,[a] Jing Yang,[a] Xinyong Chen,[a] Clive J. Roberts,[a] Ying Mei,[b] Daniel G. Anderson,[bcd] Robert Langer,[bcd] Morgan R. Alexander*[a] and Martyn C. Davies[a]

Received 7th June 2011, Accepted 21st June 2011
DOI: 10.1039/c1sm06063e

Atomic force microscopy has been applied to an acrylate polymer microarray to achieve a full topographic characterisation. This process discovered a small number of hydro-responsive materials created from monomers with disparate hydrophilicities that show reversibility between pitted and protruding nanoscale topographies.

Polymer microarrays have become a key tool for studying biological-material interactions because this format is amenable to high throughput biological assays.[1–3] Material characterisation is a key requirement of high throughput materials discovery as the property of the material cannot be determined from its composition alone, but instead requires consideration of the fabrication process.[4] Atomic force microscopy (AFM) has become the benchmark approach for nanoscale probing of surface physical properties.[5] Automated AFM surface assessment has long been applied in the quality assurance of wafers in semiconductor production plants, but much less so in a wider research context. To date the total number of samples measured in a single study was less than 90,[6–8] hence the full exploitation of the potential to use AFM to screen large scale arrays has yet to be demonstrated.

In this study a high throughput AFM characterisation methodology has been developed by the automated assessment of the surface roughness of 576 materials on a polymer microarray format. This approach included a screen for discovering materials with hydro-responsive nanotopography. The discovery of novel switchable materials is of interest for gaining temporal control of biological systems.[9,10] In addition to achieving a switchable chemical change at a surface, which has been readily observed using stimuli-responsive polymers such as poly-*N*-isopropyl acrylamide,[11] changes in surface topography have been achieved in certain material systems that were concomitant with changes in wettability and surface charge properties.[12] The temporal control of these surface properties has been used to manipulate biomolecular-surface interactions such as protein adsorption.[13–15]

A library of 22 acrylate monomers was selected to provide a wide chemical diversity likely to include materials ideally suited to fulfill a specific biological application such as controlled stem cell attachment.[16] This library included ethylene glycol chains of various length, fluoro-substituted alkanes, linear and cyclic aliphatic, aromatic and amine moieties. The array was created by mixing 16 monomers (available in the electronic supplementary information (ESI), Fig. ESI1: numbered monomers†) as the major constituent of a co-monomer mixture with 6 minor constituent monomers (Fig.-ESI1: lettered monomers†) using the same method as previously described.[1] Briefly, polymerisation solutions (75% (v/v) monomer, 25% (v/v) dimethylformamide and 1% (w/v) 2,2-dimethoxy-2-phenyl acetophenone) were deposited under a humidified argon atmosphere with the O_2 level <0.1% using a 220 μm diameter metal pin (946MP6B, Arrayit, Sunnyvale, CA, USA) onto an epoxy-coated glass slide (Genetix, San Jose, CA, USA) dip-coated with a solution of 4% (w/v) poly(hydroxyethyl methacrylate) in ethanol. Six replicates of each major monomer were included and each major monomer was mixed with each minor monomer at a ratio of 90 : 10, 85 : 15, 80 : 20, 75 : 25 and 70 : 30. This resulted in 576 polymers included in each array. After each monomer solution was printed the array was exposed to long-wave UV for 10 s and after the array had been completed for a further 30 min resulting in a polymer spot with an average diameter of 300 μm and a thickness of 17 μm. Solvent and unpolymerised monomer was subsequently removed by vacuum extraction. A standard commercial AFM (D3000A, Bruker AXS, Cambridge, UK) with a sample translation stage was optimised for fast data acquisition whilst still providing high image quality; each image of an area of 5 × 5 μm (256 lines) was acquired in approximately 3 min. Thus, for a sample set of 576 the entire array was assessed in approximately 29 h. User input during this time was

[a]*Laboratory of Biophysics and Surface Analysis, School of Pharmacy, University of Nottingham, Nottingham, UK. E-mail: Morgan.Alexander@nottingham.ac.uk*
[b]*Department of Chemical Engineering, Massachusetts Institute of Technology, Cambridge, MA, USA*
[c]*David H Koch Institute for Integrative Cancer Research, Massachusetts Institute of Technology, Cambridge, MA, USA*
[d]*Harvard-MIT Division of Health Science and Technology, Massachusetts Institute of Technology, Cambridge, MA, USA*

† Electronic supplementary information (ESI) available: the monomers used for the formation of the polymer microarray, a description of the methodology and optimisation of HT-AFM, a discussion on the correlation between material chemistry and roughness and related methods, examples of the four topographical categories observed within the microarray and the assignment of each material to a particular category, AFM images of polymers composed of monomers 16 with monomers A and B in both the dry and wet state measured by both tapping and contact mode, and a table summarising the dimensions of topographical features of copolymers of monomers 16 with monomers A and B. See DOI: 10.1039/c1sm06063e

minimal. A full description of the high throughput AFM (HT-AFM) methodology is available in the ESI (section ESI2†). Tapping mode images were acquired in both air and a liquid environment. In air, silicon tips with a resonant frequency of approximately 300 kHz and a force constant of approximately 40 N m^{-1} were used (Tap300Al, Budget Sensors, Sofia, Bulgaria). In liquid and for contact mode measurements, silicon nitride tips with a resonant frequency of approximately 7 kHz and a force constant of approximately 0.6 N m^{-1} were used (DNP-S, Bruker AXS, Cambridge, UK).

As a first pass analysis of the data, the roughness parameter R_q was used to numerically assess the sample without considering the content of the images from which this was derived. The R_q values measured in air for all materials, presented in Fig. 1a, were used to identify materials with features that deviated from the flat surface required for simple assessment of material-cell interactions. No correlation between R_q and water contact angle (WCA) was observed for this particular polymer library (See section ESI3†). The independence of roughness and surface chemistry, as sensed by WCA, was further reinforced by time-of-flight secondary ion mass spectrometry (ToF-SIMS) analysis that revealed no correlation with the polymer roughness when partial least square regression (PLS) was used (See section ESI3†). WCA and ToF-SIMS measurements and the PLS regression was conducted using methods previously described and are detailed in section ESI4†.[17–19] R_q increased proportionally with the amount of minor monomer for copolymers of 16 and A (Fig. 1b), identifying these materials for subsequent further investigation. The topographic images from the materials were then studied visually to categorise features qualitatively. Four categories of surface topography were observed across the array of 576 materials; flat surfaces, or those containing pits, nodules, or particles (have anisotropic appearance) that appeared to be sitting on a flat surface. Representative images of each of these surface types are shown in Fig. ESI6,† taken in both air and water. 486 polymer materials were categorised as flat, 16 contained pits, 44 nodules, and 30 particles. The assignment to the topographical groups for all polymers within the microarray is given in Fig. ESI6.† Pits were only observed in copolymers of monomers 16 with monomers A or B. As a relationship between R_q and minor monomer content had been observed for copolymers of 16 and A, the unique pitted topography was highlighted for further investigation. Representative topographical images from polymers composed of monomers 16 and A are shown in Fig. 2a–b and all images for compolymers within the pitted topography category are available in Fig. ESI8–9† for both the dry and wet states. Upon exposure of the surfaces to water a rapid transition from a pitted topography to protrusions was observed (Fig. 2a–b). The protrusions had a larger diameter than the pits observed in the dry state, for example, the average diameter of the protrusions across all copolymers of monomers 16 and B increased to 240 nm ± 60 nm (ranges given equal one standard deviation, n = 97) from 140 nm ± 30 nm (n = 81) for the average diameter of pits. This suggests that the content of the pits swell upon exposure to water and protrude from the background surface. The dry and wet states were imaged at different positions on the polymer's surface because the AFM probe needs to be changed when changing from imaging in air to imaging in water. However, the alignment of pits and protrusions was confirmed by subsequent contact measurements where the AFM could remain unaltered between the dry and wet states (Fig. ESI10†). In this mode the rapid swelling of the pits was observed within the time taken for the AFM to raster one line, approximately 0.3 s. Two regions were clearly observed at the surface of these materials: a flat continuum and pits or protrusions for the dry and wet states respectively. In contrast, a flat topography only was observed on the control sample: homopolymer of monomer 16 (Fig. ESI8a†).

Before polymerisation the monomers were mixed in the liquid state allowing time (*ca.* 40 min) for phase segregation for monomers with very disparate hydrophilicity. Monomer 16 has a high calculated partition constant (logP) value of 4.57 (calculated based upon their molecular structure using ACD/ChemSketch V12.01 software), compared with monomers A and B that have logP values of

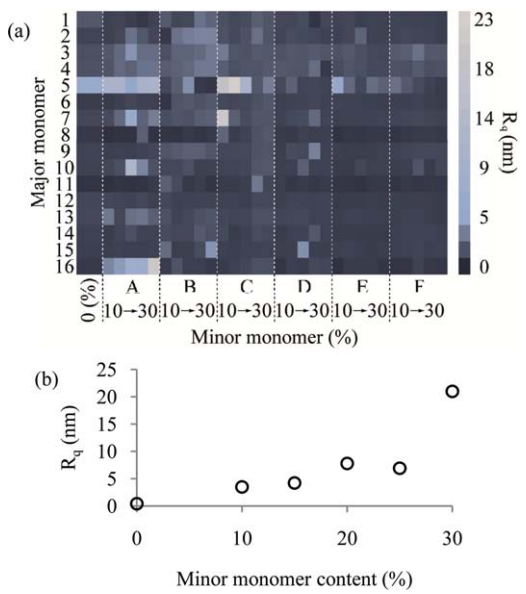

Fig. 1 (a) Intensity map of R_q (nm) for all materials represented on the array. The major monomers are listed in the *y*-axis, whilst the minor monomers at varied content are listed in the *x*-axis. (b) R_q (nm) measured on copolymers of monomer 16 and A with varied minor monomer content.

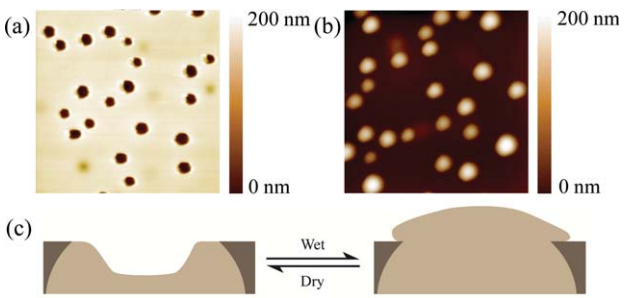

Fig. 2 AFM images taken in contact mode of polymer spots composed of 75% (v/v) monomer 16 and 25% (v/v) monomer A in (a) a dry state and (b) a wet state. All images are 5 μm × 5μm. (c) Schematic showing the transition of the phase separated copolymer switching from a pit to a protrusion. Cross-sections taken from images (a) and (b) have been used to draw the surface of these schematics. The ratio of the X and Y dimensions is accurate to 1 : 1. The hydrophobic material is shown as dark grey and the hydrophilic material is shown as light grey. The organisation of each component within the bulk is speculative.

−2.02 and −1.14 respectively, and the difference between the logP values, and therefore the hydrophilicity, of these monomers is the greatest of any combination represented in the polymer microarray. Thus, it is likely that these two monomers will be the most susceptible to phase separation prior to polymerisation, resulting in a two phase material constituted of either the pure monomers or a stable single bi-phase composition in the case that they are partially miscible. The pit number, width, coverage and corresponding R_q was measured for each pitted sample in both the dry and wet states (Table ESI1† and additional discussion). The surface coverage of the pits (dry state) increased from 9.3% ± 0.7% (n = 3) to 33.9% ± 7.6% (n = 3) with increasing minor monomer content from 10% to 30% for copolymers of monomers 16 and A (Fig. 3). The linear correlation ($R^2 = 0.89$) between surface coverage with minor monomer content suggests that the pits are composed of the hydrophilic minor monomers that swell upon exposure to water whilst the background is composed of the hydrophobic monomer 16. It is likely that spheres result in order to minimise the interface between the two phase separated areas, although the composition of the material below the surface has not been determined thus how the two phases are arranged within the bulk is speculative. This process is shown schematically in Fig. 2c. The increase in surface coverage upon immersion in water (Fig. 3) is a result of the increased diameter of protrusions compared with pits.

In order to probe the reversible change in surface topography, the pitted materials were measured again by AFM after each stage in an additional dry-wet-dry cycle. A return to a pitted topography was observed for all copolymers of monomer 16 with monomers A and B except for the copolymer composed of monomer 16 and 30% (v/v) minor monomer A (Fig. ESI8–9†). Upon drying 16A(30%) appeared to reform depressions, however, they were noticeably distorted from the original topography (Fig. ESI8f†). The large pit sizes of these materials (900 nm ± 370 nm (n = 60) average diameter for 30% (v/v) monomer A compared to 430 nm ± 120 nm (n = 60) average diameter for 25% (v/v) monomer A) could limit the material's ability to switch reversibly. The topography of a copolymer composed of monomer 16 and A (25% (v/v) minor monomer) was scanned again in wet and dry states for a second wet-dry cycle and the height and diameter was measured (Fig. 4). This demonstrated the reversible switch in nanoscale topography from pits to protrusions upon wetting after two wet-dry cycles. However, after the second cycle the depth and diameter of the pits was reduced compared to the initial dimensions (100–20 nm and 300–250 nm respectively), suggesting that some irreversible deformation of the materials occurred during the switch from pit to protrusions.

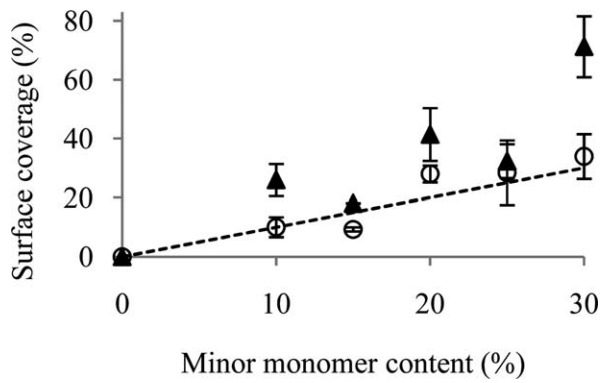

Fig. 3 Surface coverage of pits (dry) or protrusions (wet) (%) plotted *versus* minor monomer content for copolymers of 16 and A dry (○) and wet (▲) state. Error bars represent one standard deviation unit, n = 3. The y = x line is drawn as a guide.

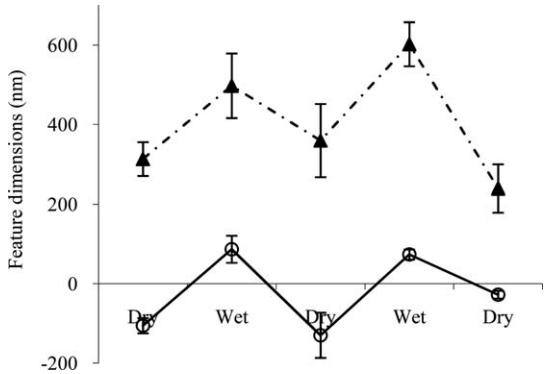

Fig. 4 The height (○) and diameter (▲) of the surface features (either pits or protrusions) imaged on the surface of polymer composed of 75% (v/v) monomer 16 and 25% (v/v) monomer A after repeated wet-dry cycles. Error bars represent one standard deviation unit, n = 20.

Solvent induced changes in nanoscale topography has been previously reported,[13,20] including a transition from pits to protrusions for a film composed of a microphase-separated block copolymer.[21] In one strategy, micelles of a block copolymer of polystyrene (PS) and poly(2-vinyl pyridine) (PVP) were prepared and coated onto a Si surface to produce an ordered array of protrusions. The block copolymer was initially solvated in toluene, which is a good solvent for PS but not for PVP, resulting in micelles with a PVP core and a PS exterior. Upon exposure to methanol, which is a good solvent for PVP but not for PS, a change in surface morphology was observed whereby an array of holes was produced with the same periodicity as the array of protrusions initially formed. Thus, either holes or protrusions could be formed on the Si substrate depending on which solvent the micelles were last exposed to.[21] The copolymer of monomers 16 and A appears to behave similarly, whereupon water is a better solvent for polymerised monomer A and air is a better 'solvent' for polymerised monomer 16.

In summary, HT-AFM has been performed on a 576 member polymer microarray to assess roughness and to classify materials by their topography. This demonstrates a key new tool for high throughput materials characterisation with which to physically characterise material microarrays. Spots with pitted topography in this library were discovered to be nano-structured hydro-responsive materials that switched between a pitted and bumpy nanoscale topography when immersed in water. This was a result of phase separation of hydrophilic monomer at the depressions dispersed as small spheres within the bulk hydrophobic monomer. This discovery is attributed to the development of HT-AFM characterisation, which allowed the investigation of roughness and topography for a library of 576 materials. Without such a large sample set it is unlikely that the materials exhibiting this interesting phenomenon (10 out of 576) would have been discovered.

Acknowledgements

Funding from the Welcome Trust (Grant number 085245/Z/08/Z) is kindly acknowledged.

Notes and references

1 D. G. Anderson, S. Levenberg and R. Langer, *Nat. Biotechnol.*, 2004, **22**, 863–866.
2 A. L. Hook, H. Thissen and N. H. Voelcker, *Langmuir*, 2009, **25**, 9173–9181.
3 S. Pernagallo, M. Wu, M. P. Gallagher and M. Bradley, *J. Mater. Chem.*, 2011, **21**, 96–101.
4 J. Kohn, *Nat. Mater.*, 2004, **3**, 745–747.
5 G. Binnig, C. F. Quate and C. Gerber, *Phys. Rev. Lett.*, 1986, **56**, 930–933.
6 D. Rende, K. Schwarz, U. Rabe, W. F. Maier and W. Arnold, *Prog. Solid State Chem.*, 2007, **35**, 361–366.
7 R. P. Herber, C. Schroter, B. Wessler and G. A. Schneider, *Thin Solid Films*, 2008, **516**, 8609–8612.
8 R. Neffati, A. Alexeev, S. Saunin, J. C. M. Brokken-Zijp, D. Wouters, S. Schmatloch, U. S. Schubert and J. Loos, *Macromol. Rapid Commun.*, 2003, **24**, 113–117.
9 B. W. Xin and J. C. Hao, *Chem. Soc. Rev.*, 2010, **39**, 769–782.
10 R. Zhang, A. Liberski, R. Sanchez-Martin and M. Bradley, *Biomaterials*, 2009, **30**, 6193–6201.
11 R. M. P. Da Silva, J. F. Mano and R. L. Reis, *Trends Biotechnol.*, 2007, **25**, 577–583.
12 I. Y. Galaev and B. Mattiasson, *Trends Biotechnol.*, 1999, **17**, 335–340.
13 A. Goel, R. G. Joshi and V. Mannari, *J. Coat. Technol. Res.*, 2009, **6**, 123–133.
14 P. C. Lin and S. Yang, *Soft Matter*, 2009, **5**, 1011–1018.
15 A. Synytska, M. Stamm, S. Diez and L. Ionov, *Langmuir*, 2007, **23**, 5205–5209.
16 Y. Mei, K. Saha, S. R. Bogatyrev, J. Yang, A. L. Hook, Z. I. Kalcioglu, S. W. Cho, M. Mitalipova, N. Pyzocha, F. Rojas, K. J. Van Vliet, M. C. Davies, M. R. Alexander, R. Langer, R. Jaenisch and D. G. Anderson, *Nat. Mater.*, 2010, **9**, 768–778.
17 M. Taylor, A. J. Urquhart, D. G. Anderson, R. Langer, M. C. Davies and M. R. Alexander, *Surf. Interface Anal.*, 2009, **41**, 127–135.
18 M. Taylor, A. J. Urquhart, M. Zelzer, M. C. Davies and M. R. Alexander, *Langmuir*, 2007, **23**, 6875–6878.
19 A. J. Urquhart, M. Taylor, D. G. Anderson, R. Langer, M. C. Davies and M. R. Alexander, *Anal. Chem.*, 2008, **80**, 135–142.
20 Y. H. Lin, J. Teng, E. R. Zubarev, H. Shulha and V. V. Tsukruk, *Nano Lett.*, 2005, **5**, 491–495.
21 S. Krishnamoorthy, R. Pugin, J. Brugger, H. Heinzelmann, A. C. Hoogerwerf and C. Hinderling, *Langmuir*, 2006, **22**, 3450–3452.